

Adjoint-based sampling methods for electromagnetic scattering

This content has been downloaded from IOPscience. Please scroll down to see the full text.

2010 Inverse Problems 26 074006

(<http://iopscience.iop.org/0266-5611/26/7/074006>)

View [the table of contents for this issue](#), or go to the [journal homepage](#) for more

Download details:

IP Address: 72.33.16.123

This content was downloaded on 05/08/2014 at 18:29

Please note that [terms and conditions apply](#).

Adjoint-based sampling methods for electromagnetic scattering

H Egger¹, M Hanke², C Schneider², J Schöberl³ and S Zaglmayr¹

¹ Institute for Computational Mathematics, Karl-Franzens-University Graz, Austria

² Institute for Mathematics, Johannes Gutenberg University, Mainz, Germany

³ Center for Computational Engineering Science, RWTH Aachen University, Germany

E-mail: herbert.egger@uni-graz.at

Received 17 December 2009, in final form 24 March 2010

Published 21 May 2010

Online at stacks.iop.org/IP/26/074006

Abstract

In this paper we investigate the efficient realization of sampling methods based on solutions of certain adjoint problems. This adjoint approach does not require the explicit knowledge of the Green's function for the background medium, and allows us to sample for all points and all dipole directions simultaneously; thus, several limitations of standard sampling methods are relieved. A detailed derivation of the adjoint approach is presented for two electromagnetic model problems, but the framework can be applied to a much wider class of problems. We also discuss a relation of the adjoint sampling method to standard backprojection algorithms, and present numerical tests that illustrate the efficiency of the adjoint approach.

1. Introduction

Electromagnetic prospection deals with the determination of electric or magnetic inhomogeneities in a known background medium. Typical problems are the localization of conducting objects from scattered electromagnetic waves, or the reconstruction of conductivity or permittivity distributions inside a body from measurements of electrostatic or quasistatic fields. Such problems arise in many applications ranging from the detection of buried landmines or the identification of airplanes by radar, to medical imaging and nondestructive testing. For details and further applications, we refer to [1, 6].

In this paper, we consider two model problems, namely the scattering of time harmonic electromagnetic waves from perfectly conducting objects and the effect of paramagnetic inclusions on magnetostatic fields. The corresponding inverse problems then consist of determining the areas of the inclusions from near field measurements of the electromagnetic fields. In principle, these nonlinear ill-posed problems can be solved by standard methods, such as the nonlinear Tikhonov regularization. However, such black-box approaches typically require heavy computations, and therefore linearizations or other approximations

are frequently used in order to facilitate fast reconstructions. The resulting schemes then naturally suffer from these approximations, and therefore have a limited range of applicability.

An alternative class of methods, established over the past years for a variety of problems, are linear sampling and probe methods, cf, e.g. [16, 21, 26], and the references therein. These methods allow us to test whether a point or a region belongs to a scattering object, without the need to iteratively solve forward problems for different parameter constellations. Therefore, sampling and probe methods enable rapid reconstructions, at least in principle. The methods we have in mind are based on range criteria of the following form:

$$g_{z,p} \in \mathcal{R}(L) \quad \text{if and only if} \quad z \in D.$$

Here, the operator L stems from a factorization of the measurement operator [11, 20], and D denotes the support of the scatterer. The test functions $g_{z,p}$ are related to a fundamental solution or Green's function for the underlying problem with singularity at a point z , and typically depend on an additional parameter (vector) p , which can be chosen in order to improve the results. The test, whether $g_{z,p}$ is in the range of a compact operator L , can be realized by Picard's criterion: if $\{\sigma_j, u_j, v_j\}$ denotes the singular system of L , then $g_{z,p} \in \mathcal{R}(L)$ if and only if

$$\sum_j \sigma_j^{-2} |(g_{z,p}, v_j)|^2 < \infty. \quad (1)$$

The efficient implementation of a range test thus requires (i) a singular value decomposition of the operator L , which for our problems can be directly related to the measurements and typically can be computed easily; (ii) the fast evaluation of the scalar products $(g_{z,p}, v_j)$, which requires the explicit knowledge of a fundamental solution for the problem under investigation. We also would like to remark that other methods, e.g. the MUSIC algorithm [9, 19] or the linear sampling method [5], rely on the knowledge and fast evaluation of Green's functions or fundamental solutions [7, 16].

In this paper, we present an alternative evaluation formula for the integrals $(g_{z,p}, v_j)$, which does not require an explicit representation of the Green's function, and additionally offers significant advantages for a numerical implementation of the sampling method. The main result of our paper will be an identity of the form

$$(g_{z,p}, v_j) = p \cdot V_j(z), \quad (2)$$

where the functions V_j can be computed directly from the singular vectors v_j of the measurement operator. This formula does not require the knowledge of the Green's function; moreover, the dependence on the parameter p is made explicit, which allows us to compute the range criterion easily for all parameter vectors p and all possible test points z , as soon as the functions V_j have been computed. As we will outline in section 5, the computation of the functions V_j (and of the measurements corresponding to the background) can be prepared offline in a pre-processing step. The evaluation of the range criterion (1) for all sampling points z and dipole directions p then only requires

- one singular value decomposition for the measurement operator,
- assembling the precomputed fields/potentials to generate the functions V_j ,
- adding the terms on the right-hand side of (2) according to (1).

We will present this *adjoint* approach in detail for two electromagnetic model problems. The approach is however applicable to a much wider class of problems, and we will give some comments in this direction in additional remarks. Let us also mention an ongoing project in electric impedance tomography, where we are using this adjoint approach successfully to

implement the factorization method of impedance tomography [15] for real data corresponding to a cylindrical object geometry, cf [10].

The explicit use of the background Green's function can also be avoided in sampling methods based on *reciprocity gap functionals* [2–4, 23]. In contrast to our approach, however, which aims for a different and more efficient implementation of the standard linear sampling method, the methods based on reciprocity gap functionals are not mathematically equivalent to the standard linear sampling method. In addition, to the best of our knowledge, these approaches still require the evaluation of a range test (i.e. the solution of certain regularized problems) for each sampling point. Thus, from an algorithmic point of view, they are closer to traditional implementations of sampling methods.

The outline of this paper is as follows: in section 2, we investigate the electromagnetic scattering from a perfect conductor. After introducing the relevant equations, we recall some details of the factorization and the linear sampling method, and then derive an identity of the form (2). In section 3, we consider a magnetostatic model problem, for which the factorization method provides somewhat stronger results, and again derive an identity of the form (2). In section 4, we establish a connection between the factorization method and backprojection methods, i.e. we show that in some cases, the linear sampling method can be interpreted as a nonlinear backprojection algorithm. This implies that linear sampling and backprojection methods can easily be integrated into one algorithm, which then provides additional quantitative information, that is usually missing in sampling methods. We conclude with presenting results of numerical experiments that illustrate the efficiency of our adjoint approach.

2. Electromagnetic scattering from a perfect conductor

The propagation of time-harmonic electromagnetic fields generated by a current source \mathcal{J}_S in a medium with constant permeability μ_0 is described by Maxwell's equations

$$\operatorname{curl} \mathcal{E} = i\omega\mu_0\mathcal{H}, \quad \operatorname{curl} \mathcal{H} = (\sigma - i\omega\epsilon)\mathcal{E} + \mathcal{J}_S. \quad (3)$$

Here, \mathcal{E} and \mathcal{H} are the complex amplitudes of the electric and magnetic fields, respectively, the functions ϵ and σ denote the permittivity and conductivity distributions of the background medium, and ω is the angular frequency. If the current source \mathcal{J}_S is locally supported, and the medium is homogeneous outside a sufficiently large ball (i.e. $\epsilon(x) = \epsilon_0$, $\sigma(x) = 0$ for $|x| \geq R'$), then the electromagnetic fields satisfy the Silver–Müller radiation condition

$$\lim_{|x| \rightarrow \infty} (\sqrt{\mu_0}\mathcal{H} \times x - |x|\sqrt{\epsilon_0}\mathcal{E}) = 0. \quad (4)$$

For a numerical realization, it is often advantageous to restrict the computational domain to a bounded set, in which case the radiation condition has to be replaced by an appropriate boundary condition. In the following we will only consider problems restricted to a large ball $\Omega = \{x \in \mathbb{R}^3 : |x| < R\}$ with $R > R'$, and we replace the radiation condition by an absorbing boundary condition [22, section 1.2]

$$\nu \times \mathcal{H} + \sqrt{\epsilon_0/\mu_0}(\nu \times \mathcal{E}) \times \nu = 0 \quad \text{on } \partial\Omega, \quad (5)$$

where ν denotes the outward pointing unit normal vector on $\partial\Omega$. Instead of this local boundary condition, one might as well consider nonlocal, exact boundary conditions based on Calderon maps [22, section 9.4].

For the rest of this section, we shall further assume that the electric parameters ϵ and σ of the background medium are piecewise constant, i.e. we assume that $\epsilon = \epsilon'$ and $\sigma = \sigma'$ in some smooth domain $\Omega' \subset \Omega$ and $\epsilon = \epsilon_0$ and $\sigma = 0$ outside Ω' ; here, $\epsilon', \epsilon_0 > 0$ and

$\sigma' \geq 0$ are the known constants. This assumption simplifies our presentation, as we can refer to the results of other papers. For some possible extensions, see the remarks at the end of this section. Finally, we assume that the source currents J_S are supported on a smooth open surface $S \subset \Omega \setminus \overline{\Omega'}$, and thus the material is homogeneous in the vicinity of S . For a sketch of the geometry, we refer to figure 1 in section 5.

2.1. Governing equations and basic notation

Let the smooth domain $D \subset \Omega'$ be the support of a perfectly conducting inclusion. By the usual scaling $E = \sqrt{\epsilon_0} \mathcal{E}$, $J_S = i\omega\mu_0\sqrt{\epsilon_0}\mathcal{J}_S$, and after elimination of the magnetic field \mathcal{H} , the scaled electric field can be seen to satisfy

$$\operatorname{curl} \operatorname{curl} E - k^2 n(x) E = J_S \quad \text{in } \Omega \setminus \overline{D}, \quad (6)$$

$$\nu \times E = 0 \quad \text{on } \partial D, \quad (7)$$

where the (positive) wave number k is defined by $k^2 = \epsilon_0\mu_0\omega^2$, the function $n(x) = \epsilon_0^{-1}[\operatorname{Im}\sigma(x)/\omega + \epsilon(x)]$ denotes the refractive index of the background and the letter ν is used to denote the unit (outward) normal, for both D and Ω . According to our remarks above, the system (6)–(7) is complemented by the absorbing boundary condition

$$\nu \times \operatorname{curl} E + ik(\nu \times E) \times \nu = 0 \quad \text{on } \partial\Omega. \quad (8)$$

Note that the case $\Omega = \mathbb{R}^3$ can be considered similarly, if (8) is replaced by a radiation condition or a non-local boundary condition [22]. Unique solvability of the boundary value problem (6)–(8) follows with standard arguments, cf [22, section 4]. The following result also holds for the special case $D = \emptyset$.

Lemma 1. *For any $J_S \in TH^{-1/2}(\operatorname{div}, S) \cap TL^2(S)$, the problem (6)–(8) has a unique solution $E \in H(\operatorname{curl}, \Omega \setminus \overline{D})$ that depends continuously on the data J_S .*

Here, $TL^2(S) = \{v \in L^2(S) : v \cdot \nu = 0\}$ denotes the space of square integrable tangential vector fields, and $TH^{-1/2}(\operatorname{div}, S) := \{v \in TH^{-1/2}(S) : \operatorname{div}_S v \in H^{-1/2}(S)\}$ is the space of functions with well-defined surface divergence; $H(\operatorname{curl}, \Omega) = \{v \in L^2(\Omega) : \operatorname{curl} v \in L^2(\Omega)\}$ denotes the space of functions with square integrable curl. For functions $v \in H(\operatorname{curl}, \Omega)$ the trace of the tangential components $(v \times \nu) \times \nu$ belongs to $TH^{-1/2}(\operatorname{curl}, \partial\Omega)$, which is the dual space of $TH^{-1/2}(\operatorname{div}, \partial\Omega)$. For details regarding these function spaces we refer to [22].

2.2. The scattering problem

As usual we decompose the total field $E = E^i + E^s$, where the incident field E^i satisfies (6) with $D = \emptyset$ and (8). By linearity of the equations, the scattered field $E^s = E - E^i$ then solves the system

$$\operatorname{curl} \operatorname{curl} E^s - k^2 n(x) E^s = 0 \quad \text{in } \Omega \setminus D, \quad (9)$$

$$\nu \times E^s = -\nu \times E^i \quad \text{on } \partial D, \quad (10)$$

$$\nu \times \operatorname{curl} E^s + ik(\nu \times E^s) \times \nu = 0 \quad \text{on } \partial\Omega. \quad (11)$$

Existence and uniqueness of the solutions E and E^i follow directly from lemma 1, and the result for E^s is obtained by $E^s = E - E^i$. Note that since n was assumed to be piecewise constant, the incident field E^i has analytic components in Ω' [6, section 6], and consequently

$\nu \times E^i|_{\partial D}$ is well defined and smooth. With the same arguments, it follows that E^s has analytic components in $\Omega \setminus \overline{\Omega'}$, and the tangential trace $\nu \times E^s|_S$ is a well-defined function in $TL^2(S)$. This allows us to define the measurement operator

$$M : TH^{-1/2}(\text{div}, S) \cap TL^2(S) \rightarrow TL^2(S), \quad J_S \mapsto (\nu \times E^s|_S) \times \nu, \quad (12)$$

that assigns to any surface excitation current J_S , the corresponding tangential component of $E^s|_S$ of the scattered electric field. The following properties of the measurement operator are direct consequences of the definition of the fields E^i and E^s .

Lemma 2. *The operator M can be extended to a compact linear operator mapping from $TL^2(S) \rightarrow TL^2(S)$. Moreover, there holds the decomposition $M = LG$, where $G : TL^2(S) \rightarrow TH^{-1/2}(\text{div}, \partial D)$ and $L : TH^{-1/2}(\text{div}, \partial D) \rightarrow TL^2(S)$ are linear compact operators defined by $G : J_S \mapsto \nu \times E^i|_{\partial D}$, and $L : -\nu \times E^i|_{\partial D} \mapsto (\nu \times E^s|_S) \times \nu$.*

Proof. The result was proven in [13] for the magnetic field formulation and unbounded domains, but the methods of proof carry over verbatim to the case considered here. The proof relies on *a priori* bounds for solutions E^i and E^s and the continuity of the tangential trace map. The compactness of the operator follows from the regularity of the scattered field; since the medium is assumed to be piecewise homogeneous we know (cf [6, section 6]) that E^s has analytic components in the vicinity of S . The result then follows by compact embedding. \square

2.3. A linear sampling method

Let $\mathbb{G}(x, z)$ denote the Green's tensor corresponding to the problem (6)–(8) with $D = \emptyset$, i.e. for any $p \in \mathbb{R}^3$ the function $G_{z,p} = \mathbb{G}(\cdot, z)p$ is a solution of

$$\text{curl curl } G_{z,p} - k^2 n(x) G_{z,p} = \delta_z p \quad \text{in } \Omega \quad (13)$$

$$\nu \times \text{curl } G_{z,p} + ik(\nu \times G_{z,p}) \times \nu = 0 \quad \text{on } \partial\Omega, \quad (14)$$

in the sense of distributions. The first equation implies that for any sufficiently smooth E satisfying $\text{curl curl } E - k^2 n(x) E = 0$ in some ball $B_r(z) = \{x \in \mathbb{R}^3 : |x - z| < r\} \subset \Omega$, there holds

$$E(z) \cdot p = \int_{\partial B_r(z)} (\nu \times \text{curl } G_{z,p} \cdot E - \nu \times \text{curl } E \cdot G_{z,p}) \, ds. \quad (15)$$

This formula follows directly from the definition of the Green's function and integration by parts, cf [22, theorem 3.31].

Remark 1. For $n \equiv 1$ in Ω , the representation (15) is just a consequence of the Stratton–Chu formula, cf [22, theorem 12.2]. In this case, the function $G_{z,p}$ can be constructed explicitly: let

$$\Phi(x, z) = \frac{1}{4\pi} \frac{e^{ik|x-z|}}{|x-z|}, \quad x \neq z$$

denote the fundamental solution of the Helmholtz equation, and

$$\tilde{\mathbb{G}}(x, z) = \Phi(x, z)\mathbb{I} + k^{-2} \nabla_z \nabla_z \Phi(x, z)$$

be the dyadic Green's function for Maxwell's equations [22, section 12]. Denote $\tilde{G}_{z,p} = \tilde{\mathbb{G}}(x, z)p$; then the solution $G_{z,p}$ of (13)–(14) is given by $G_{z,p} = \tilde{G}_{z,p} + V_{z,p}$ where $V_{z,p}$ solves (9) in Ω with boundary conditions

$$\nu \times \text{curl } V_{z,p} + ik(\nu \times V_{z,p}) \times \nu = -\nu \times \text{curl } \tilde{G}_{z,p} - ik(\nu \times \tilde{G}_{z,p}) \times \nu$$

on $\partial\Omega$. This implies that $G_{z,p}$ satisfies the homogeneous boundary condition (14).

The following result has been derived in slightly different form in [13] for the magnetic field formulation; see also [14] for corresponding results for the electric field formulation.

Lemma 3. *Let us define the test function $g_{z,p} := (v \times G_{z,p}|_S) \times v$. Then a point z belongs to D if and only if $g_{z,p} \in \mathcal{R}(L)$, with L as defined in lemma 2.*

Proof. The proof is similar to the one in [14]; the boundary condition (14) is used to take care of the bounded domain. \square

Together with the factorization stated in lemma 2, we obtain the following (weak) characterization of the inclusion.

Corollary 1. *Let $p \neq 0$. If $g_{z,p} \in \mathcal{R}(M)$, then $z \in D$.*

Since the operator M is compact, it has a singular value decomposition, and the range criterion is equivalent to the Picard criterion. This yields the following formulation of the range test, which can efficiently be used in numerical computations.

Corollary 2. *Let $\{\sigma_j, u_j, v_j\}$ denote a singular system of M and $p \neq 0$. Then the condition $\sum_j \sigma_j^{-2} |(g_{z,p}, v_j)_S|^2 < \infty$ implies $z \in D$.*

Here and below, $(u, v)_S = \int_S u \cdot \bar{v} \, ds$ denotes the L^2 scalar product of complex vector fields.

Remark 2. The arguments used in lemma 2 and corollaries 1 and 2 hold for more general inhomogeneous background media. However, the numerical realization of a sampling method based on corollary 2 requires the knowledge of the Green's function, or at least a fundamental solution of the underlying problem. Note that other sampling methods typically require the knowledge of fundamental solutions as well, cf [7]. This restricts the applicability of many sampling methods essentially to the case of homogeneous or sufficiently simple background media, and to very basic geometries.

2.4. An adjoint method

The sampling method discussed in the previous section relies on the efficient computation of the integrals $(g_{z,p}, v_j)_S$. In practice, this evaluation has to be carried out for many points z and possibly several dipole directions p . In other words, this requires the computation of the Green's function for every test point z and certain dipole directions p . In the following, we present a method that allows us to compute these integrals without an explicit knowledge of the corresponding Green's function.

For a given $v_j \in TH^{-1/2}(\text{div}, S) \cap TL^2(S)$, let V_j be the solution of the adjoint problem:

$$\text{curl curl } V_j - k^2 \bar{n}(x) V_j = v_j \quad \text{in } \Omega \quad (16)$$

$$v \times \text{curl } V_j - ik(v \times V_j) \times v = 0 \quad \text{on } \partial\Omega. \quad (17)$$

Existence and uniqueness of a solution $V_j \in H(\text{curl}, \Omega)$ of (16)–(17) is again provided by lemma 1. The following identity then follows readily by utilizing the definitions of the Green's function and the solution of the adjoint problem.

Theorem 1. *Let $g_{z,p}$ be defined as above. Then for any $v_j \in TH^{-1/2}(\text{div}, S) \cap TL^2(S)$ and $z \in \Omega \setminus S$ there holds*

$$(g_{z,p}, v_j)_S = p \cdot \overline{V_j}(z),$$

where V_j denotes the solution of (16)–(17).

Proof. Let $B_r(z) = \{x \in \Omega : |x - z| \leq r\}$ be the unit ball around z with sufficiently small radius, and denote the outer normal of $B_r(z)$ by ν again. Using (16)–(17) and $g_{z,p} = (\nu \times G_{z,p}|_S) \times \nu$, we find that

$$\begin{aligned} (g_{z,p}, v_j)_S &= (\text{curl } G_{z,p}, \text{curl } V_j)_{\Omega \setminus B_r(z)} - (G_{z,p}, k^2 \bar{n}(x) V_j)_{\Omega \setminus B_r(z)} \\ &\quad - (G_{z,p}, \nu \times \text{curl } V_j)_{\partial B_r(z)} + (G_{z,p}, ik(\nu \times V_j) \times \nu)_{\partial \Omega} \\ &= - (G_{z,p}, \nu \times \text{curl } V_j)_{\partial B_r(z)} + (\nu \times \text{curl } G_{z,p}, V_j)_{\partial B_r(z)} = p \cdot \bar{V}_j(z), \end{aligned}$$

where the last equality follows from the Stratton–Chu formula (15). \square

The alternative representation of the integrals provides the basis for a formulation of the sampling method without reference to the Green’s function.

Corollary 3. Let $\{\sigma_j, u_j, v_j\}$ denote a singular system of M , and let V_j be defined by (16)–(17). Then $g_{z,p} \in \mathcal{R}(M)$ if and only if $\sum_j \sigma_j^{-2} |p \cdot V_j(z)|^2 < \infty$.

Remark 3. Let us emphasize that this alternative formulation enables us to realize the range test for all points in the computational domain at once, as soon as the solutions V_j to the adjoint problems have been computed. As we will indicate in section 5, this can essentially be done in a pre-processing step, cf remark 14.

Due to the explicit dependence on the direction p , we can easily compute the integrals $(g_{z,p}, v_j)_S$ for several or even all directions.

Corollary 4. Let $g_{z,p}$ and V_j be defined as above. Then

$$\int_{|p|=1} |(g_{z,p}, v_j)_S|^2 dp = \frac{4\pi}{3} |V_j(z)|^2.$$

Remark 4. The statement of corollary 3 does not change if the terms $|p \cdot V_j(z)|$ are replaced by $|V_j(z)|$. Note, however, that for the electromagnetic scattering problem, the sampling method of corollary 1, respectively its equivalent formulation of corollary 3, allows us to characterize a subset $D' \subset D$ of the inclusion, only. Thus the use of several dipole directions p and the separate evaluation of the range criterion for different directions may increase the area of D' , and thus provide a better estimate of the scatterer.

Remark 5. By replacing $n(x)$ by $n(x) + n_D$ in (9), valid then in all of Ω , and by dropping (10) accordingly, we arrive at the problem of scattering from a dielectric inclusion. The adjoint system (16)–(17) remains unchanged, and the identity stated in theorem 1 holds verbatim. The corresponding identities for acoustic scattering can be derived easily by replacing the curl curl operator by the Laplacian. The generalizations to impedance or optical tomography follows similarly, cf e.g. [10].

Remark 6. Assume that Green’s function G_z with singularity at z is replaced by a mollified version $G_z^m := \int m(z) G_z dz$. Then, one obtains from theorem 1 $(g_{z,p}^m, v_j)_S = \int_{\Omega} m(z) p \cdot \bar{V}_j(z) dz$. Similarly, one can sample with the derivatives of the Green’s function and obtain identities with the corresponding derivatives of V_j . An example of the second kind will be discussed in the next section.

Remark 7. Symmetries or invariances in the measurement setup and the problem geometry can be utilized in the solution of the adjoint equations (16)–(17). For example, for a radially symmetric arrangement of sources and detectors, and a constant or radially symmetric background, only one adjoint solution has to be solved; the other solutions can then be derived from this one by using the symmetry. Similar considerations hold if the medium is stratified.

3. A scattering problem in magnetostatics

Let us now turn to a second model problem, for which the factorization method provides a sharper characterization of the domain occupied by the inclusion. Since the magnetic field is now static, all function spaces and inner products will be real in the following.

3.1. Problem formulation

For $\omega = 0$, Maxwell's equations describing the magnetic field in a linear medium with inhomogeneous permeability μ read

$$\operatorname{curl} \mathcal{H} = \mathcal{J}_S, \quad \operatorname{div}(\mu \mathcal{H}) = 0.$$

The second equation allows us to represent the magnetic induction $\mu \mathcal{H}$ by a vector potential, which we denote by \mathcal{E} again, i.e. $\mu \mathcal{H} = \operatorname{curl} \mathcal{E}$. Since adding a gradient field $\nabla \phi$ to the vector potential does not change the magnetic field \mathcal{H} , one can require \mathcal{E} to satisfy additional *gauging* conditions. In the following, we utilize a Coulomb gauge, which forces \mathcal{E} to be orthogonal to gradient fields, i.e. \mathcal{E} has to be weakly divergence free. As a consequence of the first equation, \mathcal{J}_S has to be (weakly) divergence free as well. After rescaling $E = \mu_0^{-1} \mathcal{E}$ and by rewriting $J_S = \mathcal{J}_S$, we obtain

$$\operatorname{curl} \gamma_r \operatorname{curl} E = J_S, \quad \operatorname{div} E = 0 \quad \text{in } \Omega, \quad (18)$$

where γ_r denotes the relative reluctivity defined by $\gamma_r = \mu_0/\mu$. As in the previous section, let Ω be a sufficiently large ball, and assume that $\gamma_r \equiv 1$ near $\partial\Omega$. We then complement (18) by homogeneous boundary conditions

$$\nu \times \operatorname{curl} E = 0, \quad \nu \cdot E = 0 \quad \text{on } \partial\Omega. \quad (19)$$

In the following, we assume for ease of presentation that the background medium has constant reluctivity, i.e. $\gamma_r \equiv \gamma_0$ in $\Omega \setminus D$ for some constant γ_0 ; for simplicity we assume that $\gamma_0 = 1$. Moreover, we assume that the paramagnetic inclusion has a strictly smaller constant reluctivity, i.e. $\gamma_r \equiv \gamma_1$ in D with $0 < \gamma_1 < \gamma_0$. As in the previous section, we suppose that the excitation current J_S is supported on a smooth surface $S \subset \Omega \setminus \overline{D}$; for a sketch of the geometry see figure 1 in section 5.

The unique solvability of the equations describing the magnetostatic vector potential follows from standard arguments, cf [8, chapter IX].

Lemma 4. *For any divergence free surface current $J_S \in TL_0^2(S) = \{v \in TL^2(S) : \int_S v \cdot \nabla \phi \, ds = 0 \text{ for all } \phi \in C^\infty(\Omega)\}$, the problem (18)–(19) has a unique solution $E \in H(\operatorname{curl}, \Omega)$ depending continuously on J_S .*

The total field $E = E^i + E^s$ can again be decomposed into an incident field E^i that solves (18)–(19) with $\gamma_r \equiv \gamma_0$, and a scattered field E^s , which is due to the inhomogeneity, and satisfies

$$\operatorname{curl} \gamma_r \operatorname{curl} E^s = \operatorname{curl}(\gamma_0 - \gamma_r) \operatorname{curl} E^i, \quad \operatorname{div} E^s = 0 \quad \text{in } \Omega \quad (20)$$

$$\nu \times \operatorname{curl} E^s = 0, \quad \nu \cdot E^s = 0 \quad \text{on } \partial\Omega. \quad (21)$$

Unique solvability of this problem follows from lemma 4 applied to E and E^i and the representation $E^s = E - E^i$. Note that for $\gamma_r = \gamma_0$, the scattered field vanishes.

3.2. The measurement operator and an associated factorization method

In the following, we define a measurement operator, which associates to any divergence free current J_S the corresponding trace of the tangential components of the scattered field.

Remark 8. For the results below, we have to factor out tangential traces of gradient fields, i.e. functions in $N(S) = \text{closure}\{(v \times \nabla \phi|_S) \times v : \phi \in C^\infty(\Omega)\}$, where the closure is taken with respect to $TL^2(S)$. We thus consider any $v \in TL^2(S)$ as representant for the equivalence class $v + N(S)$ in the factor space $TL^2(S)/N(S)$. This space can be identified with the dual space $TL_0^2(S)'$ of the space of divergence free tangential fields. For details, we refer to [12, 14].

Lemma 5. Let us define the current-to-measurement map

$$\tilde{M} : TL_0^2(S) \rightarrow TL_0^2(S)', \quad J_S \mapsto (v \times E^s|_S) \times v,$$

and let $\iota : TL_0^2(S) \rightarrow TL_0^2(S)'$ denote the Riesz isomorphism from $TL_0^2(S)$ into its dual. Then the measurement operator $M := \iota^{-1} \tilde{M}$ is a compact, self-adjoint linear operator on $TL_0^2(S)$.

Proof. Apart from the self-adjointness, the result was proven in [14] for the operator $\iota M \iota^{-1} = \tilde{M} \iota^{-1}$ in the case of an unbounded domain. The methods of proof, however, also apply for the situation considered here. To see that M is self-adjoint, let $J_1, J_2 \in TL_0^2(S)$, and observe that

$$(\tilde{M} J_1, J_2)_S = (\gamma_r \text{curl } E_1^s, \text{curl } E_2^s)_\Omega = (J_1, \tilde{M} J_2)_S,$$

which then implies the self-adjointness of M . \square

Remark 9. The restriction of the measurements $(v \times E^s|_S) \times v$ to the factor space $TL_0^2(S)'$, and the subsequent identification of this space with $TL_0^2(S)$ via the Riesz isomorphism amounts to a projection of the measurements onto the divergence free subspace $TL_0^2(S)$. Details concerning this projection are given in the next section.

For a characterization of the domain occupied by the inclusion, we utilize functions related to the Green's tensor for the magnetostatic equation. Here we define $G_{z,p}$ as a solution of the problem

$$\text{curl } \gamma_0 \text{curl } G_{z,p} = \text{curl}(\delta_z p), \quad \text{div } G_{z,p} = 0 \quad \text{in } \Omega \quad (22)$$

$$v \times \text{curl } G_{z,p} = 0, \quad v \cdot G_{z,p} = 0 \quad \text{on } \partial\Omega \quad (23)$$

in the sense of distributions.

Remark 10. For the case of a homogeneous background medium, e.g. $\gamma_0 \equiv 1$, the Green's function $G_{z,p}$ can be constructed explicitly. Let us define

$$\tilde{G}_{z,p}(x) = \frac{1}{4\pi} \text{curl} \frac{p}{|x - z|},$$

and let $V_{z,p}$ solve (18) with $J_S = 0$ and boundary conditions

$$v \times \text{curl } V_{z,p} = -v \times \text{curl } \tilde{G}_{z,p}, \quad v \cdot V_{z,p} = -v \cdot \tilde{G}_{z,p} \quad \text{on } \partial\Omega.$$

Then $G_{z,p} = \tilde{G}_{z,p} + V_{z,p}$ satisfies (22)–(23). The arguments below are, however, also valid for more general background media.

The following result, which is the core of the factorization method considered here, has been proven in [14] for the case of unbounded domains. The corresponding result for bounded domains follows with the same arguments.

Lemma 6. *For some $p \in \mathbb{R}^3$, let us define the test function $g_{z,p} := (v \times G_{z,p}|_S) \times v$. Then $\iota^{-1}g_{z,p} \in \mathcal{R}(|M|^{1/2})$, if and only if $z \in D$.*

The compactness of the measurement operator and the Picard criterion yield the following range test, which can efficiently be used in computations.

Corollary 5. *Let $\{\lambda_j, v_j\}$ denote an eigensystem of M , and let $g_{z,p}$ be defined as above. Then $z \in D$ if and only if $\sum_j |\lambda_j|^{-1} |(g_{z,p}, v_j)_S|^2 < \infty$.*

Proof. Since $v_j \in TL_0^2(S)$, we have $(g_{z,p}, v_j)_S = (\iota^{-1}g_{z,p}, v_j)_S$, where we identified the function $g_{z,p}$ with the corresponding distribution. The result then follows from lemma 6. \square

An application of corollary 5 requires the efficient evaluation of the inner products $(g_{z,p}, v_j)_S$, which in turn relies on the availability of an explicit representation of the Green's function, or, at least, a fundamental solution for the problem under investigation. As for the electromagnetic scattering problem considered in the previous section, one can compute these integrals without knowledge of the Green's function, by utilizing solutions to certain adjoint problems.

3.3. Adjoint formulation

Let us consider the following adjoint problem, where v_j is a divergence free tangential current source:

$$\operatorname{curl} \gamma_0 \operatorname{curl} V_j = v_j, \quad \operatorname{div} V_j = 0, \quad \text{in } \Omega \quad (24)$$

$$v \times \operatorname{curl} V_j = 0, \quad v \cdot V_j = 0 \quad \text{on } \partial\Omega. \quad (25)$$

The unique solvability of this problem for any $v_j \in TL_0^2(S)$ follows from lemma 4. For the solutions V_j of this adjoint problem, the following identities can be derived.

Theorem 2. *For given $v_j \in TL_0^2(S)$, let V_j denote the solution of (24)–(25). Then for every $p \in \mathbb{R}^3$ we have*

$$(g_{z,p}, v_j)_S = p \cdot \operatorname{curl} V_j(z),$$

where $g_{z,p}$ is defined as above. Moreover, there holds the identity

$$\int_{|p|=1} |(g_{z,p}, v_j)_S|^2 dp = \frac{4\pi}{3} |\operatorname{curl} V_j(z)|^2.$$

Proof. By the definition of V_j and $g_{z,p}$, we obtain

$$\begin{aligned} (g_{z,p}, v_j)_S &= -(\gamma_0 G_{z,p}, v \times \operatorname{curl} V_j)_{\partial B_r(z)} + (\gamma_0 v \times \operatorname{curl} G_{z,p}, V_j)_{\partial B_r(z)} \\ &= p \cdot \operatorname{curl} V_j(z), \end{aligned}$$

where the last equality follows from the definition of $G_{z,p}$ and integration by parts as in (15). The second identity then follows from integration over the unit sphere. \square

As a direct consequence of this result, we obtain the following equivalent formulation of the range test, which does not rely on an explicit representation of the Green's function.

Corollary 6. *Let $\{\lambda_j, v_j\}$ denote an eigensystem of the measurement operator M , and let V_j be defined by (24)–(25). Then a point z belongs to the inclusion D , if and only if $\sum_j |\lambda_j|^{-1} |\operatorname{curl} V_j(z)|^2 < \infty$.*

Remark 11. The results of this section can be generalized to a non-homogeneous background. However, we feel that already for the case of a homogeneous background, the alternative range test of corollary 6 has many advantages, as it allows us to sample efficiently for all points z and all directions p , as soon as the solutions V_j to the adjoint problems are available.

4. A connection to linear backprojection

In this section, we would like to highlight a connection of the adjoint formulations of the sampling methods discussed so far, to linear backprojection, which can be considered to be a first step of nonlinear Landweber iteration or other iterative regularization methods, cf e.g. [17, 18].

4.1. Forward operators

Let us consider the magnetostatic scattering problem with the constant background medium, i.e. $\gamma_r \equiv \gamma_0$ in $\Omega \setminus \overline{D}$, as discussed in the previous section, and recall that the scattered field $E_J^s(\gamma)$ corresponding to a source J and the relative reluctivity distribution γ_r satisfies

$$\begin{aligned} \operatorname{curl} \gamma_r \operatorname{curl} E_J^s &= \operatorname{curl} (\gamma_0 - \gamma_r) \operatorname{curl} E_J^i, & \operatorname{div} E_J^s &= 0 & \text{in } \Omega, \\ \nu \times \operatorname{curl} E_J^s &= 0, & \nu \cdot E_J^s &= 0 & \text{in } \partial\Omega, \end{aligned}$$

where the incident field $E_J^i(\gamma)$ is given by

$$\operatorname{curl} \gamma_0 \operatorname{curl} E_J^i = J, \quad \operatorname{div} E_J^i = 0 \quad \text{in } \Omega \quad (26)$$

$$\nu \times \operatorname{curl} E_J^i = 0, \quad \nu \cdot E_J^i = 0 \quad \text{in } \partial\Omega. \quad (27)$$

We define a nonlinear operator $\tilde{F}_J : \mathcal{D}(F) \rightarrow TL_0^2(S)'$ that maps the reluctivity distribution to the (equivalence class of) measurements $(\nu \times E_J^s|_S) \times \nu$ of the scattered field corresponding to a specific source current J . As in lemma 5, we then define the forward operator $F_J := \iota^{-1} \tilde{F}_J$, where $\iota : TL_0^2(S) \rightarrow TL_0^2(S)'$ is the Riesz isomorphism.

Remark 12. For $u \in TL^2(S)$, we define the restriction $\Pi : u \mapsto u - \nabla_S \phi$, where ∇_S denotes the surface gradient, and $\phi \in H^1(S)$ solves the variational problem

$$(\nabla_S \phi, \nabla_S \psi)_S = (u, \nabla_S \psi)_S \quad \text{for all } \psi \in C^\infty(\Omega).$$

It follows that $\Pi u \in TL_0^2(S)$ for any $u \in TL_0^2(S)$; see also remark 9. We then have $F_J(\gamma) = \Pi((\nu \times E_J^s|_S) \times \nu)$, and obtain $F_J(\gamma) = MJ$, where M is the measurement operator defined in lemma 5.

The derivative of the forward operator F at γ_0 in direction h is given by $F'_J(\gamma_0)h = \Pi((\nu \times W_J^s|_S) \times \nu)$, where W_J^s is the solution of

$$\operatorname{curl} \gamma_0 \operatorname{curl} W_J^s = -\operatorname{curl} h \operatorname{curl} E_J^i, \quad \operatorname{div} W_J^s = 0 \quad \text{in } \Omega, \quad (28)$$

$$\nu \times \operatorname{curl} W_J^s = 0, \quad \nu \cdot W_J^s = 0 \quad \text{in } \partial\Omega. \quad (29)$$

The action of the adjoint of the derivative operator on some element $r \in TL_0^2(S)$ is then given by

$$\begin{aligned}(F'_J(\gamma_0)^* r, h)_{L^2(\Omega)} &= (r, F'_J(\gamma_0)h)_{TL^2(S)} = (r, (v \times W_J^s) \times v)_{TL^2(S)} \\ &= (\gamma_0 \operatorname{curl} E_r^i, \operatorname{curl} W_J^s)_{L^2(\Omega)} = -(h \operatorname{curl} E_r^i, \operatorname{curl} E_J^i)_{L^2(\Omega)},\end{aligned}$$

where E_r^i is the solution of (26)–(27) with J replaced by r , and the adjoint was taken with respect to the scalar products of $L^2(\Omega)$ and $TL^2(S)$. For $r \in TL_0^2(S)$, this yields the representation

$$F'_J(\gamma_0)^* r = -\operatorname{curl} E_r^i \cdot \operatorname{curl} E_J^i.$$

4.2. Multiple excitations

As a next step, we generalize these definitions to the case of multiple excitations. Let $M = M(\gamma_r)$ denote the measurement operator defined above corresponding to a reluctivity distribution γ_r . We then define the full forward operator $F : \gamma_r \rightarrow M(\gamma_r)$ by $F(\gamma_r)J := F_J(\gamma_r)$ for all $J \in TL_0^2(S)$.

The measurement space $\mathcal{L}(TL_0^2(S), TL_0^2(S))$ can be equipped with the Hilbert–Schmidt norm defined by $\|A\| = \sqrt{\langle A, A \rangle}$, where

$$\langle A, B \rangle = \sum_{i,j} (Av_j, Bv_i)_{TL^2(S)},$$

and $\{\lambda_j, v_j\}$ denotes an eigensystem of $M(\gamma_r)$. The action of the adjoint operator $F'(\gamma_0)^*$ on some element R in the measurement space is then defined by

$$\begin{aligned}(F'(\gamma_0)^* R, h)_{L^2(\Omega)} &= \langle R, F'(\gamma_0)h \rangle = \sum_{i,j} (Rv_j, (v \times W_{v_i}|_S) \times v)_{TL^2(S)} \\ &= -\sum_{i,j} (h \operatorname{curl} U_j, \operatorname{curl} V_i)_{L^2(\Omega)},\end{aligned}$$

where W_{v_i} is defined by (28)–(29) with J replaced by v_i , and the functions U_j and V_i solve (26)–(27) with $J = Rv_j$ and $J = v_i$, respectively. Thus the action of the adjoint derivative is given by

$$F'(\gamma_0)^* R = -\sum_{i,j} \operatorname{curl} U_j \cdot \operatorname{curl} V_i. \quad (30)$$

4.3. Linearization and backprojection

For solving the nonlinear inverse problem $F(\gamma_r) = M$, we consider a formal linearization of the forward operator

$$F(\gamma_r) = F(\gamma_0) + F'(\gamma_0)(\gamma_r - \gamma_0) + o(\|\gamma_r - \gamma_0\|),$$

and we consider the linearized problem $F'(\gamma_0)(\gamma_r - \gamma_0) = M$ (note that $F(\gamma_0) = 0$) instead of the nonlinear problem. Applying a simple linear backprojection yields as a first approximation

$$\gamma_r \sim \gamma_0 + F'(\gamma_0)^* M;$$

thus, we have to apply the adjoint of the derivative operator only to the special element $R = M$. Utilizing the fact, that v_j are the eigenvectors of M , we obtain $Rv_j = Mv_j = \lambda_j v_j$, and thus $U_j = \lambda_j V_j$. Inserting this into (30), we obtain the representation

$$F'(\gamma_0)^* M = -\sum_{i,j} \lambda_j \operatorname{curl} V_j \cdot \operatorname{curl} V_i \quad (31)$$

for the update of the linear backprojection method.

Remark 13. Note that the functions V_j are just the solutions of the adjoint problems (24)–(25), which were already used for the adjoint implementation of the factorization method. By replacing $\lambda_j \operatorname{curl} V_j$ in (31) by $-\delta_{ij} |\lambda_j|^{-1} \operatorname{curl} V_j$, we recover the sampling method of corollary 6. In any case, the functions V_j that are required for the implementation of the range test of the sampling method can be reused for the application of the backprojection; hence, both methods can be implemented easily within one algorithm.

5. Numerical tests

Let us discuss the implementation of the adjoint sampling method for the scattering from a perfect conductor. For our numerical tests, we use the following geometry: $\Omega = B_5(0)$ is the ball around the origin with radius 5. For the refractive index of the background medium, we choose $n(x) = n' = 2 + i$ in $\Omega' = B_1(0)$ and $n(x) \equiv 1$ in $\Omega \setminus \Omega'$, and the wavenumber is set to $k = 1$. The scatterer D is contained in the cube $[-0.5, 0.5]^2 \times [0.3, 0.5] \subset \Omega'$, as depicted in figure 1. Finally, the excitations and measurements are located at the surface $S = \partial B_{1.1}(0) \cap \{z \geq 0\}$.

5.1. Discretization by finite elements

For the discretization of the electric field equations, we use an $H(\operatorname{curl})$ -conforming finite element method with high order Nedgelec finite elements [25, 28] consisting of piecewise polynomials with maximal degree 5. The space $TL^2(S)$ of excitation currents and measurements is approximated by the lowest order Nedgelec space [24] restricted to the surface S ; this means that one source/detector is associated with each edge on the measurement surface S . In our numerical test example, the total number of degrees of freedom of a finite element solution is $nd = 202\,570$ and the number of independent sources/detectors is $ns = 171$. All computations were implemented in the open-source finite element software NETGEN/NGSolve [27].

A discretization of the problems (6)–(8) yields linear systems of the form

$$A(D)E_j = J_j, \quad j = 1, \dots, ns, \quad (32)$$

where $A(D)$ refers to the system matrix in the presence of a perfectly conducting scatterer located in D . The scattered fields defined by (9)–(11) with excitations J_j are then given by $E_j^s = E_j - E_j^i$, and the entries of the measurement matrix, which corresponds to a discretization of the measurement operator M , is obtained by evaluation of the tangential traces of E_j^s at the measurement surface.

5.2. Adjoint sampling method

After computing a singular value decomposition $\{\sigma_j, u_j, v_j\}$ of the $ns \times ns$ dimensional measurement matrix, we have to determine the adjoint solutions V_j of (16)–(17), which are defined by linear systems of the form

$$A(\emptyset)\overline{V_j} = \overline{v_j}, \quad j = 1, \dots, ns. \quad (33)$$

Since the problems (33) have to be solved many times for different right-hand sides, we utilized a sparse factorization of the $(nd \times nd)$ -dimensional matrix $A(\emptyset)$; the solutions of the systems (33) can then be computed very fast. The required computation times for this part of the calibration procedure are listed in table 1.

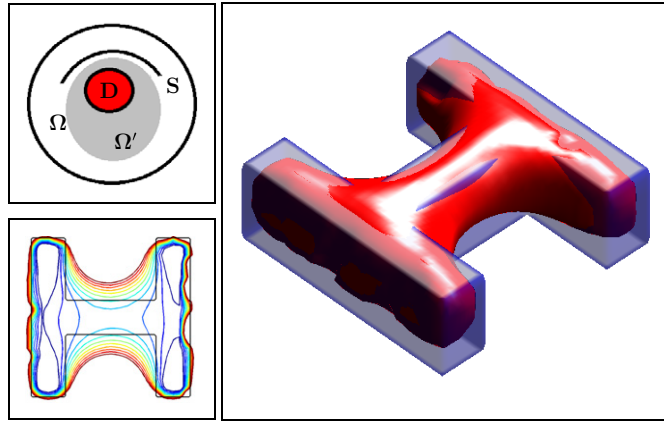


Figure 1. Top-left: sketch of the geometry. Bottom-left: isolines of the reconstruction c_n and the true object at the plane $\{(x, y, 0.4)\}$. Right: isosurface of the reconstruction c_n (red) and the domain D of the scattering object (blue).

(This figure is in colour only in the electronic version)

Remark 14. As the singular vectors $v_j = \sum_k v_{jk} J_k$ can be expressed via the sources J_k , we obtain $V_j = \sum_k v_{jk} \overline{E_k^i}$, where E_k^i denotes the solution of the forward problem without scatterer and current source J_k . Thus, no further pde problems have to be solved here to assemble the adjoint solutions V_j . In the case of real data, we can choose a basis $\{e_k : k = 1, \dots, ns\}$ of the measurement space, and determine the ns solutions E_k^i , $k = 1, \dots, ns$ of (33) with v_j replaced by e_k . Note that this computationally demanding task can be done independently of the data in a calibration step, and the functions V_j can be assembled by linear combination from E_k^i . In the presence of noise in the data, only few singular values σ_j should be used in the range test, and only the corresponding function V_j have to be assembled in practice; see below.

For a quantitative evaluation of the range criterion of corollary 3, we implement the numerical range test as follows: for z on a uniform grid and some $0 < n \leq ns$, we compute

$$s_n(z) = C(z)^{-1} \sum_{j=1}^n \sigma_j^{-2} |V_j(z)|^2,$$

where the factors $C(z) := \left(\sum_{j=1}^{ns} |V_j(z)|^2 \right) = \frac{4\pi}{3} \int_{S^2} \|g_{z,p}\|_S^2 dp$ are intended to facilitate a comparison of the resulting numbers for different sampling points with each other. In our numerical example, we chose the truncation index n by $\sigma_{n+1} < \delta \sigma_1 \leq \sigma_n$ with $\delta = 10^{-6}$, which in this case amounts to $n = 96$. (In general, the truncation level δ will depend on the noise of the data.) Alternatively, one could replace the denominator σ_j^2 by $\sigma_j^2 + \alpha$ for some $\alpha > 0$ and set $n = ns$. The isolines and isosurfaces of the function $c_n(z) = \log(s_n(z))$ are displayed in figure 1.

The overall sampling method then consists of the following steps.

(A) *Calibration*

- (i) Solution of the linear system (33) with ns right-hand sides $v_j = e_k$. Using appropriate solvers, the complexity of this part is $O(nd \times ns)$ operations.

Table 1. Computation times for A(i), solution of the system (33); A(ii), sampling of the functions E_k^i ; B(i), computing the singular value decomposition of the measurement matrix; and B(ii), evaluating the range criterion for all sampling points.

Calibration		Application	
A(i)	A(ii)	B(i)	B(ii)
Solution of (33)	eval $E_k^i(z)$	svd	Range criterion
585s	45s	0.1s	3.6s

- (ii) Evaluation and storing of the functions $E_k^i(z)$ at nz sampling points. Since the finite element basis functions have local support, the complexity of this step is $O(nz \times ns)$.

(B) *Application*

- (i) Singular value decomposition of the measurement matrix with approximately $O(ns^3)$ complexity.
- (ii) Assembling of the functions $V_j = \sum_k v_{jk} \overline{E_k^i}$ and computing the sum in the range criterion: complexity $O(ns^2 \times nz)$.

Remark 15. Let us note that instead of precomputing the functions E_k^i in a pre-processing step and then assembling the adjoint functions V_j from them, one could also compute the functions V_j directly in step B of the algorithm. This would change the computational cost of step B(ii) to $O(ns \times nd + ns \times nz)$. In our numerical experiments, pre-computing the functions E_k^i was however substantially faster; cf also table 1. The process of assembling the functions V_j from E_k^i (step B(ii)) could be further accelerated by parallelization or execution on graphics cards, such that the adjoint sampling method is actually usable for online monitoring.

The computation times required for the individual steps are summarized in table 1. The discretization using high-order Nedgelec elements utilized $nd = 202\,570$ degrees of freedom, and the number of sources/detectors was chosen to be $ns = 171$. The sampling was performed on a $50 \times 50 \times 50$ grid resulting in $nz = 125\,000$ sampling points. All computations were performed on a standard dual-core desktop PC.

For comparison, the standard implementation of the linear sampling method would have required nz solutions of linear systems similar to (33) to determine the associated Green's function. The overall computation time would then be much larger.

5.3. Discrete identity

At the end of this section, we would like to make a remark concerning the adjoint approach on the discrete level. The identities of theorem 1 and 2 also hold for discretizations in the following sense: let $V_h \subset H(\text{curl}, \Omega)$ denote a conforming finite element space, and let $G_{z,p}^h$ denote the discrete Green's function corresponding to (13)–(14), i.e. $G_{z,p}^h \in V_h$ such that

$$(\text{curl } G_{z,p}^h, \text{curl } v_h)_\Omega - k^2(n(x) G_{z,p}^h, v_h)_\Omega + ik(G_{z,p}^h, (v \times v_h) \times v)_{\partial\Omega} = p \cdot \bar{v}_h(z)$$

for all $v_h \in V_h$. Since the test functions v_h are in general not continuous on Ω , the evaluation points z have to be restricted to the interior of the individual elements. Accordingly, we define V_j^h as the solutions of the discrete adjoint problems

$$(V_j^h, v_h)_\Omega - k^2(\bar{n}(x) V_j^h, v_h)_\Omega - ik(V_j^h, (v \times v_h) \times v)_{\partial\Omega} = (v_j, v_h)_S$$

for all $v_h \in V_h$. If $g_{z,p}^h = (v \times G_{z,p}^h|_S) \times v$, then there holds

$$(g_{z,p}^h, v_j)_S = p \cdot \bar{V}_j^h(z).$$

Note that this identity in general does not hold, if $g_{z,p}^h$ is defined differently, e.g. by L^2 -projection of $g_{z,p}$ onto the finite element (trace) space.

6. Conclusion

In this manuscript, we proposed an alternative formulation of linear sampling methods, that does not require the explicit knowledge of the Green's function or a fundamental solution for the underlying problem. The resulting algorithms allow us to sample for all test points z in the domain and several dipole directions p simultaneously. Most of the computational work can be done in a pre-processing step, and the actual application of the sampling method is very fast and allows for online monitoring. The solutions of the adjoint problems, that are required for the implementation, are also used in the evaluation of forward operators and backprojection algorithms. Therefore, the adjoint sampling methods can be integrated easily within the existing code for nonlinear inverse problems. As we outlined in remarks, the adjoint approach is not restricted to the electromagnetic model problems, discussed in this paper, but can easily be generalized to a wide range of problems, e.g. in acoustic scattering, or electric impedance tomography. Moreover, similar techniques can also be utilized for the implementation of other sampling and probe methods.

References

- [1] Baum C 1999 *Detection and Identification of Visually Obscured Targets* (Philadelphia, PA: Taylor and Francis)
- [2] Collino F, Fares M'B and Haddar H 2003 Numerical and analytical studies of the linear sampling method in electromagnetic inverse scattering problems *Inverse Problems* **19** 1279–98
- [3] Cakoni F, Fares M'B and Haddar H 2006 Analysis of two linear sampling methods applied to electromagnetic imaging of buried objects *Inverse Problems* **22** 845–67
- [4] Colton D and Haddar H 2005 An application of the reciprocity gap functional to inverse scattering theory *Inverse Problems* **21** 383–98
- [5] Colton D and Kirsch A 1996 A simple method for solving inverse scattering problems in the resonance region *Inverse Problems* **12** 383–93
- [6] Colton D and Kress R 1998 *Inverse Acoustic and Electromagnetic Scattering Theory* 2nd edn (Berlin: Springer)
- [7] Colton D and Kress R 2006 Using fundamental solutions in inverse scattering *Inverse Problems* **22** R49–66
- [8] Dautray R and Lions J-L 1990 *Mathematical Analysis and Numerical Methods for Science and Technology* vol 3 (Berlin: Springer)
- [9] Devaney A J 2003 A super-resolution processing of multi-static data using time reversal and MUSIC *J. Acoust. Soc. Am.* (submitted)
- [10] Drewitz J Eine Anwendung der Faktorisierungsmethode für reale Daten von dreidimensionalen zylindrischen Tanks. *Diploma Thesis* Johannes-Gutenberg Universität Mainz, Germany (in preparation)
- [11] Gebauer B 2006 The factorization method for real elliptic problems *Z. Anal. Anwend.* **25** 81–102
- [12] Gebauer B 2006 Gebietserkennung mit der Faktorisierungsmethode *Dissertation* Universität Mainz
- [13] Gebauer B, Hanke M, Kirsch A, Muniz W and Schneider C 2005 A sampling method for detecting buried objects using electromagnetic scattering *Inverse Problems* **21** 2035–50
- [14] Gebauer B, Hanke M and Schneider C 2008 Sampling methods for low-frequency electromagnetic imaging *Inverse Problems* **24** 015007
- [15] Hanke M and Brühl M 2003 Recent progress in electrical impedance tomography *Inverse Problems* **19** S65–90
- [16] Hanke M and Kirsch A 2009 Sampling methods (manuscript)
- [17] Hanke M, Neubauer A and Scherzer O 1995 A convergence analysis of the Landweber iteration for nonlinear ill-posed problems *Numer. Math.* **72** 21–37
- [18] Kaltenbacher B, Neubauer A and Scherzer O 2008 *Iterative Regularization Methods for Nonlinear Ill-Posed Problems (Radon Series on Computational and Applied Mathematics)* (Berlin: de Gruyter)
- [19] Kirsch A 2002 The MUSIC algorithm and the factorization method in inverse scattering theory for inhomogeneous media *Inverse Problems* **18** 1025–40
- [20] Kirsch A 2004 The factorization method for Maxwell's equations *Inverse Problems* **20** S117–34

- [21] Kirsch A and Grinberg N 2008 *The Factorization Method for Inverse Problems* (Oxford: Oxford University Press)
- [22] Monk P 2003 *Finite Element Methods for Maxwell's Equations* (Oxford: Clarendon)
- [23] Monk P and Sun J 2007 Inverse scattering using finite elements and gap reciprocity *Inverse Problems Imaging* **1** 643–60
- [24] Nédélec J C 1980 Mixed finite elements in \mathbb{R}^3 *Numer. Math.* **35** 315–41
- [25] Nédélec J C 1986 A new family of mixed finite elements in \mathbb{R}^3 *Numer. Math.* **50** 57–81
- [26] Potthast R 2005 Sampling and probe methods *Computing* **75** 215–35
- [27] Schöberl J 1997 NETGEN—an advancing front 2d/3d-mesh generator based on abstract rules *Comput. Vis. Sci.* **1** 41–52
- [28] Schöberl J and Zaglmayr S 2005 High-order Nédélec elements with local complete sequence properties *COMPEL Int. J. Comput. Math. Electr. Electron. Eng.* **24** 374–84
- [29] Schenk O and Gärtner K 2004 Solving unsymmetric sparse systems of linear equations with PARDISO *Future Gener. Comput. Syst.* **20** 475–87